TABLE 1. Biochemical parameters

	Cord blood (n = 23)	Mother (n = 21)	Adult (n = 25)
Calcium (mg/dl)[a]	10.5 ± 0.43	9.44 ± 0.34[b]	9.42 ± 0.29[b]
Phosphate (mg/dl)	4.93 ± 0.65	3.66 ± 0.59[b]	3.62 ± 0.50[b]
Intact PTH (pg/ml)	7.11 ± 5.22	26.5 ± 12.2[b,f]	36.4 ± 9.80[b]
25-OHD (ng/ml)	8.95 ± 3.47	13.3 ± 6.45[d]	15.0 ± 4.43[c]
Albumin (g/dl)	3.53 ± 0.38	3.15 ± 0.42[c,e]	4.60 ± 0.27[b]
Creatinine (mg/dl)	0.49 ± 0.09	0.48 ± 0.08[e]	0.69 ± 0.10[b]

Data are expressed as mean ± SD and were compared among the cord blood group, mother group, and adult volunteer group using the ANOVA test.

[a] The calcium values were corrected using the following formula in cases involving hypoalbuminemia (Alb < 4.0 g/dl): corrected calcium (mg/dl) = measured calcium (mg/dl) + 4 − albumin (g/dl) (15).

[b] $P < 0.0001$ *vs.* cord blood; [c] $P < 0.01$ *vs.* cord blood; [d] $P < 0.05$ *vs.* cord blood; [e] $P < 0.0001$ *vs.* adult; [f] $P < 0.01$ *vs.* adult.

whereas serum intact PTH levels were lower in the cord blood than in the sera of the mother and adult volunteers (3).

The levels of soluble α-Klotho in the cord blood were markedly higher than those in the other groups ($P < 0.0001$) (Fig. 1A). The mean value for soluble α-Klotho in the cord blood was 3243 ± 1899 pg/ml, whereas those in the sera of the neonates at d 4, mothers, and adult volunteers were 582 ± 90, 768 ± 261, and 681 ± 140 pg/ml, respectively. There was no significant difference among the samples from neonates at d 4, mothers, and adults.

On the other hand, the levels of FGF23 in cord blood were significantly lower than those in other groups ($P < 0.0001$, *vs.* neonate and adult; $P < 0.0005$, *vs.* mother) (Fig. 1B). The mean value for FGF23 in cord blood was 8.61 ± 6.48 pg/ml, whereas those in the neonates, mothers, and adult volunteers were 28.4 ± 20.5, 26.7 ± 15.1, and 34.6 ± 7.69 pg/ml, respectively.

Negative correlation between the levels of soluble α-Klotho and FGF23 in cord blood samples

Then, using only the cord blood samples (n = 23), we examined the relationship between the levels of soluble α-Klotho and FGF23. We found that soluble α-Klotho levels were inversely correlated with FGF23 levels ($R^2 = 0.20$; $P < 0.05$) (Fig. 1C).

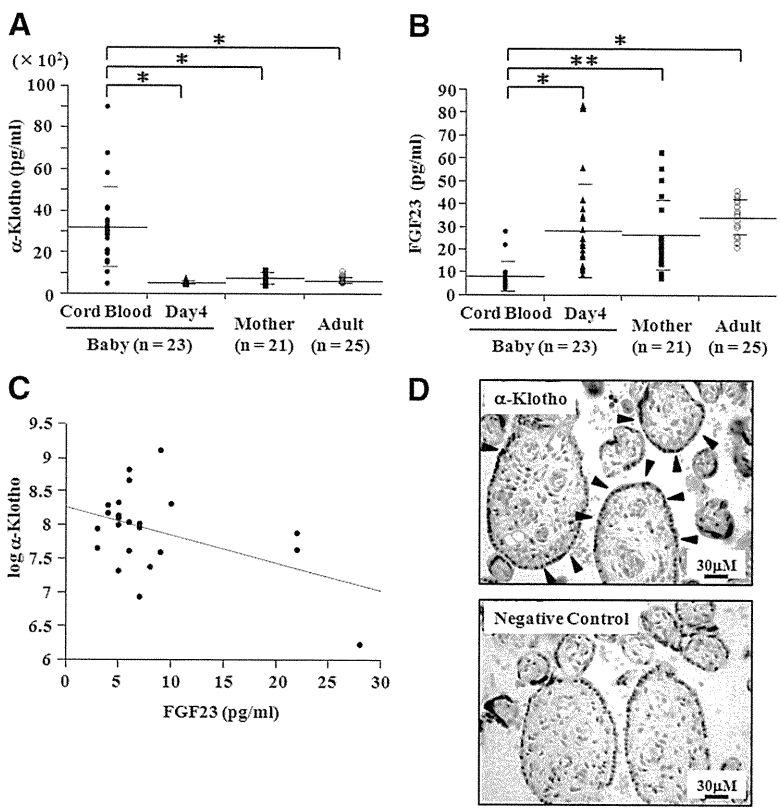

FIG. 1. A and B, Comparison of serum soluble α-Klotho (A) and FGF23 (B) levels among the cord blood, neonate at d 4, mother, and adult volunteer groups by ANOVA. *, $P < 0.0001$; **, $P < 0.0005$. *Closed circles*, *triangles*, *squares*, and *open circles* denote the values for the cord blood, neonate, mother, and adult volunteer groups, respectively. The *long and short bars* represent the mean and SD, respectively. C, Correlation of serum levels of α-Klotho with FGF23 in cord blood samples according to Pearson's correlation test. α-Klotho was log-transformed to reduce skewness. $R^2 = 0.20$; $P < 0.05$. D, Representative image of normal human term placenta stained with antibody against α-Klotho. α-Klotho was predominantly expressed in syncytiotrophoblasts (*arrowheads*). Normal goat IgG was used as a negative control.

Expression of α-Klotho in syncytiotrophoblasts in term placenta

Immunohistochemical staining demonstrated that α-Klotho was predominantly expressed in syncytiotrophoblasts with some expression in endothelium of fetal vessels and connective tissue of villi (Fig. 1D).

Discussion

In the current study, we found that the levels of soluble α-Klotho in cord vein blood that inflow to fetus after the exchange of gas and nutrients in the placenta were markedly higher than those in neonates, mothers, and adults (Fig. 1A). Immunohistochemical staining of the placenta revealed that syncytiotrophoblasts that originate from fetus predominantly expressed α-Klotho (Fig. 1D). Although we cannot exclude the possibility that other fetal tissues also contribute, it is likely that the syncytiotrophoblast is one of the major sources of the soluble α-Klotho circulating abundantly in the fetus. The lower level of soluble α-Klotho in neonates at d 4 compared with that in cord

blood supports the idea that the protein is derived from the placenta.

In contrast to the high levels of soluble α-Klotho, the levels of FGF23 in cord blood were lower than those in the other samples. This result was consistent with the findings of a previous report (17). Considering a report demonstrating that FGF23 expression in fetal rat bones was much lower than that in young adult rat bones (18), the low levels of FGF23 in cord blood might be due to the low expression of FGF23 in fetal tissues. In addition, it may suggest that the FGF23 in the mother's blood is not transferred to the fetus through the placenta.

We found a negative correlation between soluble α-Klotho and FGF23 levels in the cord blood samples. This result was also compatible with the data reported by Yamazaki *et al.* (13) in which samples from healthy children and adult volunteers were analyzed. Although the precise mechanism is unknown, the high level of soluble α-Klotho circulating in the fetus may contribute to the low level of intact FGF23 in cord blood.

We also performed multiple regression analysis and found that soluble α-Klotho was one of the determinants of the levels of phosphate (Supplemental Table 1, published on The Endocrine Society's Journals Online web site at http://jcem.endojournals.org). Serum calcium level also might be associated with that of α-Klotho, although the *P* value was 0.07. It has been reported that TRPV6 is involved in maternal-fetal calcium transport in mouse models (19). Moreover, Lu *et al.* have recently reported that α-Klotho activated not only TRPV5 but also TRPV6 (20). Given these results, soluble α-Klotho may contribute to the establishment of the fetomaternal calcium gradient also. However, considering the observation that the absence of α-Klotho in mice leads to hypercalcemia and hyperphosphatemia after birth (4), it remains to be determined whether the high levels of α-Klotho is an epiphenomenon in response to the higher serum calcium and phosphate, or is causing some of the biochemical features of fetuses. Even so, we can say that the measurement of soluble α-Klotho in cord blood as a biomarker might be useful in management of some genetic neonatal conditions such as hypercalcemia and hypophosphatemia. Measurement of calcium and phosphate during the perinatal period in the α-Klotho-deficient mice and generation of syncytiotrophoblast-specific α-Klotho-knockout mice might provide further insight into the roles of Klotho in fetal mineral metabolism.

In conclusion, the levels of soluble α-Klotho in cord blood were markedly high, and syncytiotrophoblasts in placenta were likely to be one of the major sources. Soluble α-Klotho in cord blood might be useful as a biomarker for calcium and phosphate metabolism in fetus.

Acknowledgments

We thank the staff of the neonate intensive care unit of Osaka University Hospital and all participants and their families.

Address all correspondence and requests for reprints to: Keiichi Ozono, M.D., Ph.D., 2-2 Yamadaoka, Suita, Osaka, 565-0871, Japan. E-mail: keioz@ped.med.osaka-u.ac.jp.

This work was supported by Grants-in-Aid for Scientific Research from the Japan Society for the Promotion of Science (to H.A.), Grants-in-Aid for Incurable Diseases from Osaka Medical Research Foundation for incurable diseases (to H.A.), and Grants-in-Aid for Intractable Disease from the Ministry of Health, Labor and Welfare of Japan (to T.M. and K.O.).

Disclosure Summary: Y.O., H.A., N.N., T.K., H.H., K.W., M.N., T.M., A.I., Y.N., and K.O. have nothing to declare. Y.Y. is an employee of Kyowa-Hakko Kirin Co., Ltd.

References

1. **Simmonds CS, Karsenty G, Karaplis AC, Kovacs CS** 2010 Parathyroid hormone regulates fetal-placental mineral homeostasis. J Bone Miner Res 25:594–605
2. **Kovacs CS, Lanske B, Hunzelman JL, Guo J, Karaplis AC, Kronenberg HM** 1996 Parathyroid hormone-related peptide (PTHrP) regulates fetal-placental calcium transport through a receptor distinct from the PTH/PTHrP receptor. Proc Natl Acad Sci USA 93:15233–15238
3. **Kovacs CS** 2008 Fetal calcium metabolism. In: Rosen CJ, ed. Primer on the metabolic bone diseases and disorders of mineral metabolism. 7th ed. Washington, DC: American Society for Bone and Mineral Research; 108–112
4. **Kuro-o M, Matsumura Y, Aizawa H, Kawaguchi H, Suga T, Utsugi T, Ohyama Y, Kurabayashi M, Kaname T, Kume E, Iwasaki H, Iida A, Shiraki-Iida T, Nishikawa S, Nagai R, Nabeshima YI** 1997 Mutation of the mouse klotho gene leads to a syndrome resembling ageing. Nature 390:45–51
5. **Imura A, Tsuji Y, Murata M, Maeda R, Kubota K, Iwano A, Obuse C, Togashi K, Tominaga M, Kita N, Tomiyama K, Iijima J, Nabeshima Y, Fujioka M, Asato R, Tanaka S, Kojima K, Ito J, Nozaki K, Hashimoto N, Ito T, Nishio T, Uchiyama T, Fujimori T, Nabeshima Y** 2007 α-Klotho as a regulator of calcium homeostasis. Science 316:1615–1618
6. **Chang Q, Hoefs S, van der Kemp AW, Topala CN, Bindels RJ, Hoenderop JG** 2005 The β-glucuronidase klotho hydrolyzes and activates the TRPV5 channel. Science 310:490–493
7. **Urakawa I, Yamazaki Y, Shimada T, Iijima K, Hasegawa H, Okawa K, Fujita T, Fukumoto S, Yamashita T** 2006 Klotho converts canonical FGF receptor into a specific receptor for FGF23. Nature 444:770–774
8. **The ADHR Consortium** 2000 Autosomal dominant hypophosphataemic rickets is associated with mutations in FGF23. Nat Genet 26:345–348
9. **Shimada T, Mizutani S, Muto T, Yoneya T, Hino R, Takeda S, Takeuchi Y, Fujita T, Fukumoto S, Yamashita T** 2001 Cloning and characterization of FGF23 as a causative factor of tumor-induced osteomalacia. Proc Natl Acad Sci USA 98:6500–6505
10. **Segawa H, Kawakami E, Kaneko I, Kuwahata M, Ito M, Kusano K, Saito H, Fukushima N, Miyamoto K** 2003 Effect of hydrolysis-resistant FGF23–R179Q on dietary phosphate regulation of the renal type-II Na/Pi transporter. Pflugers Arch 446:585–592
11. **Imura A, Iwano A, Tohyama O, Tsuji Y, Nozaki K, Hashimoto N, Fujimori T, Nabeshima Y** 2004 Secreted Klotho protein in sera and

CSF: implication for post-translational cleavage in release of Klotho protein from cell membrane. FEBS Lett 565:143–147
12. **Kurosu H, Yamamoto M, Clark JD, Pastor JV, Nandi A, Gurnani P, McGuinness OP, Chikuda H, Yamaguchi M, Kawaguchi H, Shimomura I, Takayama Y, Herz J, Kahn CR, Rosenblatt KP, Kuro-o M** 2005 Suppression of aging in mice by the hormone Klotho. Science 309:1829–1833
13. **Yamazaki Y, Imura A, Urakawa I, Shimada T, Murakami J, Aono Y, Hasegawa H, Yamashita T, Nakatani K, Saito Y, Okamoto N, Kurumatani N, Namba N, Kitaoka T, Ozono K, Sakai T, Hataya H, Ichikawa S, Imel EA, Econs MJ, Nabeshima Y** 2010 Establishment of sandwich ELISA for soluble α-Klotho measurement: age-dependent change of soluble α-Klotho levels in healthy subjects. Biochem Biophys Res Commun 398:513–518
14. **Yamazaki Y, Okazaki R, Shibata M, Hasegawa Y, Satoh K, Tajima T, Takeuchi Y, Fujita T, Nakahara K, Yamashita T, Fukumoto S** 2002 Increased circulatory level of biologically active full-length FGF-23 in patients with hypophosphatemic rickets/osteomalacia. J Clin Endocrinol Metab 87:4957–4960
15. **Fukumoto S, Namba N, Ozono K, Yamauchi M, Sugimoto T, Michigami T, Tanaka H, Inoue D, Minagawa M, Endo I, Matsumoto T** 2008 Causes and differential diagnosis of hypocalcemia—recommendation proposed by expert panel supported by ministry of health, labour and welfare, Japan. Endocr J 55:787–794
16. **Cunningham FG, Levono KJ, Bloom SL, Hauth JC, Rouse DJ, Spong CY** 2010 Williams obstetrics. 23rd ed. New York: McGraw-Hill
17. **Takaiwa M, Aya K, Miyai T, Hasegawa K, Yokoyama M, Kondo Y, Kodani N, Seino Y, Tanaka H, Morishima T** 2010 Fibroblast growth factor 23 concentrations in healthy term infants during the early postpartum period. Bone 47:256–262
18. **Yoshiko Y, Wang H, Minamizaki T, Ijuin C, Yamamoto R, Suemune S, Kozai K, Tanne K, Aubin JE, Maeda N** 2007 Mineralized tissue cells are a principal source of FGF23. Bone 40:1565–1573
19. **Suzuki Y, Kovacs CS, Takanaga H, Peng JB, Landowski CP, Hediger MA** 2008 Calcium channel TRPV6 is involved in murine maternal-fetal calcium transport. J Bone Miner Res 23:1249–1256
20. **Lu P, Boros S, Chang Q, Bindels RJ, Hoenderop JG** 2008 The β-glucuronidase klotho exclusively activates the epithelial Ca2+ channels TRPV5 and TRPV6. Nephrol Dial Transplant 23:3397–3402

Journal of Human Genetics (2011), 1–3

www.nature.com/jhg

COMMENTARY

Hypophosphatasia now draws more attention of both clinicians and researchers: A Commentary on prevelance of c. 1559delT in *ALPL*, a common mutation resulting in the perinatal (lethal) form of hypophosphatasias in Japanese and effects of the mutation on heterozygous carriers

Keiichi Ozono and Toshimi Michigami

Journal of Human Genetics advance online publication, 10 February 2011; doi:10.1038/jhg.2011.6

Hypophosphatsia is a skeletal disease due to an inborn error of metabolism characterized by deficient activity of the tissue-nonspecific alkaline phosphatase.[1,2] Alkaline phosphatase (ALP) is a membrane-bound metalloenzyme that consists of a group of isoenzymes encoded by four different gene loci: tissue-nonspecific, intestinal, placental and germ-cell ALP. Tissue-nonspecific alkaline phosphatase is expressed in almost all cells and three organs, liver, bone and kidney, have high activity of ALP. Thus, tissue-nonspecific alkaline phosphatase is also called ALP liver/bone/kidney (ALPL). The mouse counter part is called Akp2. Tissue-nonspecific alkaline phosphatase hydrolyzes inorganic pyrophosphate, an inhibitor of mineralization, and increases the local concentration of inorganic phosphate. Therefore, hypomineralization of skeleton and rachitic change of bone is associated with hypophosphatasia.

Hypophosphatasia is highly variable in its clinical expression. On the basis of the age of manifestation and its severity, hypophosphatasia is divided into six subtypes (Table 1). The most severe form of hypophosphatasia is a perinatal form, which is also called a lethal form. This form presents clinically either before or in the newborn period. The patients with this form exhibit severe defect of bone mineralization including craniotabes, bone deformity, short stature and narrow chest, and suffer from respiratory failure (Figure 1). However, some patients of this form can survive because of advances in neonatology.[3] Recently, non-lethal benign form of perinatal hypophosphatasia has been recognized, which is associated with no apparent defects of mineralization.[4,5] An infantile form is characterized by infantile onset and often associated with poor weight gain, hypercalcemia and respiratory difficulties. This form shows still rather high mortality. A childhood form is manifested at the age of 2 or 3 with premature loss of teeth, rachtic change of long bones and mild short stature. An adult form is sometimes associated with pathologic bone fracture and an odonto types means a form of only teeth manifestation. Diagnosis of hypophosphatasia is made on the basis of the clinical features, skeletal X-ray findings and low activity of ALP associated with elevation of its substrate, such as phosphoethanolamine, inorganic pyrophosphate and pyridoxal-5′-phosphate. We described diagnostic criteria of hypophosphatasia proposed by the Japanese Hypophosphatasia Study Group at http://www.bone.med.osaka-u.ac.jp/english/b5/.

Hypophosphatasia is usually inherited in an autosomal recessive manner, but can be expressed in an autosomal dominant manner in milder forms.[6] The *ALPL* gene is located on the short arm of chromosome 1 (1p36.1–p34), and contains 12 exons. The product consists of 507 amino acids including residues of the signal peptide. Hypophosphatasia is caused by various mutations in the *ALPL* gene. Currently, more than 200 mutations of the *ALPL* gene in patients with hypophosphatasia have been registered in the *ALPL* gene mutations database (http://www.sesep.uvsq.fr/Database.html). Most mutations described to date are missense mutations (80%), and the remainder was several deletion and insertion mutations of one to four nucleotides. Large deletions of the gene are rare (1.3%). Correlations of genotype and phenotype have been reported on the basis of clinical data of the patients with hypophosphatasia, enzymatic activity and computer-assisted modeling.[2]

We previously reported that the most and the second-most frequent mutations in Japanese patients are T1559del and F310L, respectively.[5] These mutations are renamed to c.1559delT and p.F327 L, respectively, based on the recent standardized nomenclature. Interestingly, both mutations are unique to Japanese. The common mutations, c.1559delT and p.F327 L, are associated with lethal and the perinatal non-lethal forms of hypophosphatasia, respectively. This is an example of

Professor K Ozono is at the Department of Pediatrics, Osaka University Graduate School of Medicine, 2-2 Yamadaoka, Suita, Osaka 565-0871, Japan and T Michigami is at the Department of Bone and Mineral Research Osaka Medical Center and Research Institute for Maternal and Child Health, 840 Murodo-cho, Izumi, Osaka 594-1101, Japan.
E-mail: keioz@ped.med.osaka-u.ac.jp

Table 1 Subtypes of hypophosphatasia and features

Subtypes	*Onset*	*Features*
Perinatal lethal	Fetus, neonate	Respiratory failure, severe mineralization defect, convulsion
Perinatal non-lethal	Fetus, neonate	Bone deformity
Infantile	Infant	Failure to thrive, hypercalcemia
Childhood	Child, especially toddlers	Premature loss of teeth, rickets-like changes
Adult	Adulthood	Fragile bone
Odonto	Not indicated	Teeth involvement only

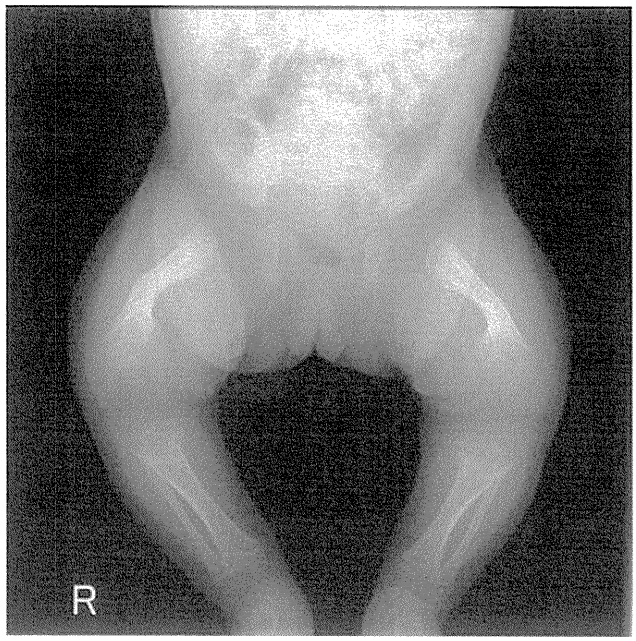

Figure 1 X-ray of legs of a neonate of hypophosphatasia. Severe rachitic changes of metaphysis of long bones are characteristic to hypophosphatasia. Bone deformity is also recognized.

the genotype–phenotype relationship, consistent with the enzymatic activity of the mutant ALP proteins; c.1559delT caused a complete loss of activity, whereas p.F327 L retains some residual activities. Therefore, genotyping patients with hypophosphatasia may help to predict their prognosis. In Europe, the E174K (renamed to p.E191K) mutation is reported to be frequent with a frequency of 31% in patients with mild hypophosphatasia.[7] As the E174K is associated with the same rare haplotype, the E174K mutation is surmised to be an ancestral mutation. However, the allele frequency of the E174K mutation is not investigated in normal population. In this issue of the journal, Watanabe *et al.*[8] reported prevelance of c. 1559delT in *ALPL*, a common mutation resulting in the perinatal (lethal) form of hypophosphatasias in Japanese. According to the article, the frequency is one per 480 (1/480), resulting in 1/920 000 homozygotes, because *de novo* mutation seems extremely rare. The frequency indicates more than one patient with this homozygous mutation is born per year in Japan, which has ~1 100 000 newborns per year. In our experience of examination of mutation in the *ALPL* gene in 42 patients with hypophosphatasia, homozygous mutation of c.1559delT was found in 17% patients. Thus, around seven patients with hypophosphatasia per year may be born in Japan based on the small number of examination. The carrier frequency for the mutant allele is estimated to be 1/25 in the Manitoba Mennonite community in Canada, which has the highest incidence rate for severe form of hypophosphatasia.[9]

There is no established medical treatment to cure hypophosphatasia, but there are some specific treatments for complications of hypophosphatasia.[1] In severe form of hypophosphasia, patients often suffer from intractable convulsions. This complication was also reported in $akp2^{-/-}$ mice.[10] The convulsion can be controlled by administration of vitamin B6 because abnormal metabolism of vitamin B6 leading to the deficient γ-aminobutyric acid in brain is observed in $akp2^{-/-}$ mice. In an infantile form of hypophosphatasia, patients tend to have hypercalcemia because of low bone formation. Low calcium-containing milk is recommended for hypercalcemia. Recently, treatment with parathyroid hormone 1–34, teriparatide, has been reported to improve bone formation, although its effect is still controversial.[11,12] Bone marrow transplantation has been reported to treat several patients with hypophosphatasia.[13] However, a method must be developed that improves the survival of donor mesenchymal cells in patients. Likewise, other congenital enzyme defect disorders, such as Hurler or Hunter disease, recombinant enzyme replacement therapy is being attempted in hypophosphatasia. Recombinant bone-targeted ALP therapy is effective in terms of mineralization and life-span in $akp2^{-/-}$ mice.[14] The therapy is now on clinical trial and expected to be available in near future.

1 Whyte, M. P. Physiological role of alkaline phosphatase explored in hypophosphatasia. Prolonged survival and phenotypic correction of Akp2(−/−) hypophosphatasia mice by lentiviral gene therapy. *Ann. N. Y. Acad. Sci.* **1192,** 190–200 (2010).
2 Mornet, E. Hypophosphatasia. *Orphanet. J. Rare. Dis.* **2,** 40 (2007).
3 Nakamura-Utsunomiya, A., Okada, S., Hara, K ., Miyagawa, S., Takeda, K., Fukuhara, R. *et al.* Clinical characteristics of perinatal lethal hypophosphatasia: a report of 6 cases. *Clin. Pediatr. Endocrinol.* **19,** 7–13 (2010).
4 Stevenson, D. A., Carey, J. C., Coburn, S. P., Ericson, K. L., Byrne, J. L., Mumm, S. *et al.* Autosomal recessive hypophosphatasia manifesting in utero with long bone deformity but showing spontaneous postnatal improvement. *J. Clin. Endocrinol. Metab.* **93,** 3443–3448 (2008).
5 Michigami, T., Uchihashi, T., Suzuki, A., Tachikawa, K., Nakajima, S. & Ozono, K. Common mutations F310L and T1559del in the tissue-nonspecific alkaline phosphatase gene are related to distinct phenotypes in Japanese patients with hypophosphatasia. *Eur. J. Pediatr.* **164,** 277–282 (2005).
6 Müller, H. L., Yamazaki, M., Michigami, T., Kageyama, T., Schönau, E., Schneider, P. *et al.* Asp361Val mutant of alkaline phosphatase found in patients with dominantly inherited hypophosphatasia inhibits the activity of the wild-type enzyme. *J. Clin. Endocrinol. Metab.* **85,** 743–747 (2000).
7 Hérasse, M., Spentchian, M., Taillandier, A. & Etienne, M. Evidence of a founder effect for the tissue-nonspecific alkaline phosphatase (TNSALP) gene E174K mutation in hypophosphatasia patients. *Eur. J. Hum. Genet.* **10,** 666–668 (2002).
8 Watanabe, A., Karasugi, T., Sawai, H., Naing, B. T., Ikegawa, S., Orimo, H. *et al.* Prevalence of c.1559delT in *ALPL*, a common mutation resulting in the perinatal (lethal) form of hypophosphatasia in Japanese and effects of the mutation on heterozygous carriers. *J. Hum. Genet.* (e-pub ahead of print 23 December 2010; doi:10.1038/jhg.2010.161).
9 Greenberg, C. R., Taylor, C. L., Haworth, J. C., Seargeant, L. E., Philipps, S., Triggs-Raine, B. *et al.* A homoallelic Gly317–>Asp mutation in ALPL causes the perinatal (lethal) form of hypophosphatasia in

Canadian mennonites. *Genomics.* **17**, 215–217 (1993).
10 Fedde, K. N., Blair, L., Silverstein, J., Coburn, S. P., Ryan, L. M., Weinstein, R. S. *et al.* Alkaline phosphatase knock-out mice recapitulate the metabolic and skeletal defects of infantile hypophosphatasia. *J. Bone. Miner. Res.* **14**, 2015–2026 (1999).
11 Whyte, M. P., Mumm, S. & Deal, C. Adult hypophosphatasia treated with teriparatide. *J. Clin. Endocrinol. Metab.* **92**, 1203–1208 (2007).
12 Gagnon, C., Sims, N. A., Mumm, S., McAuley, S. A., Jung, C., Poulton, I. J. *et al.* Lack of sustained response to teriparatide in a patient with adult hypophosphatasia. *J. Clin. Endocrinol. Metab.* **95**, 1007–1012 (2010).
13 Whyte, M. P., Kurtzberg, J., McAlister, W. H., Steele, A., Coburn, S. P., McAlister, W. H. *et al:* Marrow cell transplantation for infantile hypophosphatasia. *J. Bone. Miner. Res.* **18**, 624–636 (2003).
14 Millán, J. L., Narisawa, S., Lemire, I., Loisel, T. P., Boileau, G., Leonard, P. *et al.* Enzyme replacement therapy for murine hypophosphatasia. *J. Bone. Miner. Res.* **23**, 777–787 (2008).

JBC Papers in Press. Published on November 12, 2010 as Manuscript M110.148403
The latest version is at http://www.jbc.org/cgi/doi/10.1074/jbc.M110.148403

Cellular ATP synthesis mediated by type III sodium-dependent phosphate transporter *Pit-1* is critical to chondrogenesis

Atsushi Sugita[1, 5], Shinji Kawai[2], Tetsuyuki Hayashibara[3], Atsuo Amano[2], Takashi Ooshima[3], Toshimi Michigami[4], Hideki Yoshikawa[5], Toshiyuki Yoneda[1]

[1]Department of Biochemistry, [2]Department of Oral Frontier Biology, [3]Department of Pediatric Dentistry, Osaka University Graduate School of Dentistry, [4]Department of Bone and Mineral Research, Osaka Medical Center and Research Institute for Maternal and Child Health, Izumi, Osaka 594-1101, Japan, [5]Department of Orthopaedic Surgery, Osaka University Graduate School of Medicine, 1-8 Yamadaoka, Suita-Osaka 565-0871, Japan.

Running head: *Pit-1* regulation of late chondrogenesis

Address correspondence to: Toshiyuki Yoneda, D.D.S., Ph.D. 1-8 Yamadaoka, Suita-Osaka 565-0871, Japan. Fax: +81-6-6879-2890: E-mail: tyoneda@dent.osaka-u.ac.jp

Disturbed endochondral ossification in X-linked hypophosphatemia (XLH) indicates an involvement of phosphate (Pi) in chondrogenesis. We studied the role of the sodium-dependent Pi co-transporters (NPT), which are a widely-recognized regulator of cellular Pi homeostasis, and its downstream events in chondrogenesis using *Hyp* mice, the murine homologue of human XLH. *Hyp* mice showed reduced apoptosis and mineralization in hypertrophic cartilage. *Hyp* chondrocytes in culture displayed decreased apoptosis and mineralization compared with wild-type (WT) chondrocytes, while glycosaminoglycan synthesis, an early event in chondrogenesis, was not altered. Expression of the type III NPT *Pit-1* and Pi uptake were diminished and intracellular ATP levels were also reduced in parallel with decreased caspase-9 and caspase-3 activity in *Hyp* chondrocytes. The competitive NPT inhibitor phosphonoformic acid (PFA) and ATP synthesis inhibitor 3-bromopyruvate (3-BrPA) disturbed endochondral ossification with reduced apoptosis *in vivo* and suppressed apoptosis and mineralization in conjunction with reduced Pi uptake and ATP synthesis in WT chondrocytes. Overexpression of *Pit-1* in *Hyp* chondrocytes reversed Pi uptake and ATP synthesis and restored apoptosis and mineralization. Our results suggest that cellular ATP synthesis consequent to Pi uptake via *Pit-1* plays an important role in chondrocyte apoptosis and mineralization and that chondrogenesis is ATP-dependent.

Endochondral ossification is critical to the development and growth of mammalians. The process begins with condensation of undifferentiated mesenchymal cells and these cells differentiate into proliferating chondrocytes which express type II, type IX, type XI collagen and sulfated glycosaminoglycans (GAG) (1). Proliferating chondrocytes further differentiate into hypertrophic chondrocytes expressing type X collagen, undergo apoptosis, mineralize and ultimately replaced by bone. Disturbance of the endochondral ossification leads to a variety of skeletal disorders.

The genetic disease X-linked hypophosphatemia (XLH) is the most common form of inherited rickets in humans and is related to the dominant disorder of phosphate (Pi) homeostasis (2). XLH is shown to be caused by inactive mutations of the *PHEX* gene and characterized by hypophosphatemia secondary to renal Pi wasting, growth retardation due to disturbed endochondral ossification, osteomalacia resulting from reduced mineralization and abnormally-regulated vitamin D metabolism (3). *Hyp* mice also display similar biochemical and phenotypic abnormalities with human XLH including hypophosphatemia, osteomalacia and skeletal abnormalities. *Hyp* mice thus are a mouse homologue of the human XLH (4). Previous studies reported that *Hyp* mice exhibited disorganized hypertrophic cartilage with reduced apoptotic chondrocytes and hypomineralization (5). We have previously reported that osteoclast number was decreased in *Hyp* mice compared with wild-type (WT) mice and high-Pi diet partially restored this, showing that Pi influences osteoclastogenesis and suggesting this Pi effect on osteoclastogenesis may be associated with the pathogenesis of abnormal skeletogenesis in *Hyp* mice (6). However, it remains unclear whether disturbed Pi homeostasis influences endochondral ossification leading to abnormal skeletogenesis in *Hyp* mice. In this context, it is noted that intracellular Pi levels decrease and extracellular Pi

levels prominently increase from the proliferating to the hypertrophic zone during chondrogenesis (7-10), suggesting that cellular Pi levels are associated with chondrocyte differentiation.

Cellular Pi levels are controlled by the sodium-dependent Pi co-transporters (NPT) (11). Previous studies reported that the type III NPT (*Pit-1*) was expressed in hypertrophic chondrocytes during endochondral ossification in mice (12) and that the expression of the type IIa NPT (*Npt2a*) and *Pit-1* was also detected in chick chondrocytes (13). Moreover, it has been demonstrated that Pi modulates chondrocyte differentiation (14-19) and apoptosis (13,20).

Based on these earlier results, we hypothesized that the NPT/Pi system plays a critical role in the regulation of chondrocyte differentiation. We found that *Pit-1* expression in chondrocytes is decreased in *Hyp* mice compared to WT mice and that *Pit-1* regulates apoptosis and mineralization in chondrocytes through modulating intracellular ATP synthesis and apoptotic signaling activity. On the other hand, *Hyp* chondrocytes showed no changes in GAG synthesis, which is an early event in chondrogenesis. Our findings suggest that ATP synthesis mediated by Pi influx via *Pit-1* is critical in the regulation of late chondrogenesis including apoptosis and mineralization and that the differentiation of cartilage is an ATP-dependent event.

EXPERIMENTAL PROCEDURES

Animals - All mice used were of the C57BL/6J strain. Normal mice were purchased from Nihon-Dobutsu Inc. (Osaka, Japan). *Hyp* mice were initially obtained from The Jackson Laboratory (Bar Harbor, ME), and were produced by cross-mating homozygous *Hyp* females (*Hyp*/*Hyp*) to hemizygous *Hyp* males (*Hyp*/Y). All animal experiments were performed according to the guideline of the Institutional Animal Care and Use Committee of Osaka University Graduate School of Dentistry.

Isolation and culture of mouse growth plate chondrocytes - Growth plate chondrocytes were isolated from the ribs of 4-week-old normal and *Hyp* mice by sequential digestion with 0.2% trypsin (Invitrogen, Carlsbad, CA) for 30 minutes and 0.2% collagenase (Wako Pure Chemical Industries Ltd. Osaka, Japan) for 3 hours as previously report (21). Isolated cells were plated onto 100-mm tissue culture dishes at a density of $1x10^6$ cells in α-minimum essential medium (α-MEM: Sigma, St. Louis, MO) supplemented with 10% FCS (Valley Biomedical Inc., Winchester, VA), 2 mmol/L L-glutamine and 0.1 mg/mL kanamycin. Two days later, to induce chondrogenesis and cartilage nodule formation, cells were plated at $3x10^5$ cells/well onto 24-well plates or at $5x10^4$ cells/well on 96-well plates coated with type I collagen (Nitta Gelatin Inc, Osaka, Japan) and cultured in the differentiation medium consisting of Dulbecco's modified Eagle medium (DMEM: Sigma) supplemented with 10% FCS, 50 μg/mL ascorbic acid and 100 ng/mL recombinant human bone morphogenetic protein-2 (rhBMP-2, Astellas Pharma Inc. Tokyo, Japan) for 7 days. From day 5 to day 7, to promote matrix mineralization, 5 mM β-glycerophosphate was added to the differentiation medium.

Reverse transcription-polymerase chain reaction (RT-PCR) and real-time PCR - Total RNA from chondrocytes was prepared using RNeasy kit (QIAGEN Inc., Valencia, CA) and reverse-transcribed with SuperScript II reverse transcriptase (Invitrogen). The primer sequences for mouse Npt1, mouse Npt2a, GAPDH and β-actin are available on request. PCR assays were performed using Taq DNA Polymerase (New England Biolabs Inc., Ipswich, MA) and dNTP Mix (Promega Corp. Madison, WI). Real-time PCR assays were performed using a LightCycler system (Roche Diagnostics) according to the manufacturer's instructions. Each reaction was carried out with QIAGEN QuantiTect SYBR Green PCR Master Mix. The expression levels of mRNA are indicated as the relative expression normalized by GAPDH. The primer sequences are available on request. Each procedure was repeated at least four times to assess reproducibility.

Measurement of Na-dependent Pi uptake - Assay for Na-dependent Pi uptake by growth plate chondrocytes was performed essentially as described (22). Briefly, confluent cells cultured in 24 well Costar microtiter dishes were incubated in 2 ml of uptake solution (150 mmol/L NaCl, 1.0 mmol/L $CaCl_2$, 1.8 mmol/L $MgSO_4$, 10 mmol/L HEPES, pH 7.4) at 37°C for 5 min. Transport was then initiated by replacing the uptake solution with fresh uptake solution (2 ml), supplemented with 0.1 mmol/L KH_2PO_4, and containing 3 μCi/mL of $KH_2{}^{32}PO_4$ (MP Biomedicals Inc, Irvine, CA). Cells were then incubated for 5 min at 37°C, and the reaction was stopped by the addition of ice-cold uptake solution supplemented with 150 mmol/L choline chloride substitution for NaCl. The same solution was then used to wash the cells three times (2 ml per wash), dissolved in 0.2 N NaOH, and the ^{32}P activity was counted on a scintillation counter. As a control, Na-independent Pi transport was measured in the same way, except that NaCl was

replaced by choline chloride in the uptake solution. Data were expressed as nanomoles of Pi per milligram of cellular protein per 5 min and Na-dependent Pi transport was calculated by subtracting Na-independent Pi transport from total Pi transport.

Alcian blue staining - Cell layers in 24-well plates were fixed with 3.7% formaldehyde for 10 minutes and with 70% ethanol for 5 minutes at room temperature. After fixation, cells were incubated with 5% acetic acid (pH 1.0 adjusted with HCl) for 5 minutes and stained with 1% alcian blue dye (Wako Pure Chemical Industries Ltd.) in 5% acetic acid for 10 minutes. The alcian blue staining was quantified using an NIH Image 1.63 software.

Alizarin red staining - Cell layers in 24-well plates were fixed with 3.7% formaldehyde for 10 minutes and with 95% ethanol for 10 minutes at room temperature. After fixation, mineralized nodules were stained with 1% alizarin red-S (Wako Pure Chemical Industries Ltd.) at pH 6.4 for 10 minutes at room temperature. The stained samples were washed three times with water and then air dried. The alizarin red staining was quantified using an NIH Image 1.63 software.

Treatment with NPT inhibitor - In vitro: Chondrocytes were treated with phosphonoformic acid (PFA or foscarnet, Sigma), which is a competitive inhibitor of NPT (23), at concentrations of 10^{-5} M to 10^{-3} M in the differentiation medium from day 1 to day 7. *In vivo*: Mice received PFA as described (24). PFA injection (*ip*, 1,000 mg/kg body weight) was started at 21-day-old and daily injected for 10 days into C57BL/6J mice. Histological analysis was performed at 31-day-old. Control mice received vehicle PBS.

Knockdown of Npt2a and Pit-1 by siRNA - Chondrocytes were seeded at a density of $5x10^5$ cells in 100-mm tissue culture dishes in α-MEM supplemented with 10% FCS and 2 mmol/L L-glutamine. The sequences of Stealth RNAi duplex oligoribonucleotides for mouse *Npt*2a and mouse *Pit-1* are available on request. *Npt2a*-targeted, *Pit-1*-targeted, or negative control (medium GC, siNEGATIVE, Invitrogen) Stealth RNAi duplex oligoribonucleotides was added to 1 mL serum-free Opti-MEM I Reduced-Serum Medium (Invitrogen) in a final concentration of 24 nM respectively. In a separate tube 20 μL Lipofectamine RNAiMAX (Invitrogen) were diluted in 1 mL serum-free Opti-MEM I Reduced-Serum Medium. After adding the siRNA solution to the Lipofectamine solution, the final transfection mixture was incubated for 20 min at room temperature. This transfection mixture was applied to the cells. After 48 hours, RNA extraction was performed for RT-PCR and transfected chondrocytes were plated onto 24-well plates or 96-well plates to determine Pi-transport, intracellular ATP levels, caspase activity and apoptosis.

Pit-1 overexpression - The cDNA was subcloned into the 5'-XhoI-BamHI-3' site of pcDNA3.1/Zeo (Invitrogen). Cells were transfected using FuGENE™-6 (Roche Diagnostics Inc) according to the manufacturer's protocol. After 48 hours of transfection, RNA extraction was performed for RT-PCR or transfected chondrocytes were re-plated onto 24-well plates or 96-well plates to determine Pi-transport, intracellular ATP levels, caspase activity and apoptosis. The cDNA for mouse *Pit-1* in the plasmid pBluescript was a generous gift of Dr. Kenichi Miyamoto (University of Tokushima Graduate School, Tokushima, Japan).

Histology and TUNEL staining - Tibiae were harvested, washed with PBS, fixed with 4% paraformaldehyde in 0.1 M phosphate buffer (pH 7.4) overnight, decalcified in 4.13% EDTA at room temperature for 2 weeks, and embedded in paraffin. Four-micrometer-thick sections were made and stained with hematoxylin and eosin. Apoptotic cells were identified by using the DeadEnd Fluorometric TUNEL System (Promega Corp.). After treatment with 10 mg/mL proteinase K for 10 min at room temperature, sections were incubated with rTdT incubation buffer for 1 hour at 37°C, rinsed, counterstained with 1 μg/mL 4',6-Diamidino-2-phenylindole (DAPI, Vector Laboratories, Ltd., Burlingame, CA) and mounted with Fluoromount-G (Southern Biotechnology Associates Inc, Birmingham, AL). The green TUNEL emission was analyzed under fluorescein filter set to view the green fluorescence of fluorescein at 520 nm and blue DAPI at 460 nm.

Measurement of apoptotic cell death - DNA fragmentation was measured using Cell Death Detection ELISA PLUS kit (Roche Diagnostics Inc), which detects the cytoplasmic histone-associated DNA fragments (mono- and oligonucleosomes) by photometric enzyme-immunoassay. Briefly, after differentiation of chondrocytes in 96-well plates, cell lysates were used for ELISA procedure, following the manufacture's protocol. DNA fragmentation was quantified at 405 nm. Results were normalized to cellular protein concentration.

Measurement of caspase-9 and caspase-3 activity - Activity of caspase-3 and caspase-9 was measured using the Caspase-Glo 3/7 Assay kit (Promega) and the Caspase-Glo 9 Assay kit (Promega) according to the manufacturer's instructions. Chondrocytes were cultured at a density of 5 x 10^4 cells/well for 5 days in 96-well plates in the differentiation medium and processed for caspase-9 and caspase-3 activity assays. The luminescence was measured using a luminometer (TD-20/20, Tuner Designs, Sunnyvale, CA). Results were normalized to cellular protein concentration.

Measurement of intracellular ATP levels - Intracellular ATP levels were measured by using ATP Assay kit (Calbiochem, Darmstadt, Germany). This assay utilizes luciferase to catalyze the formation of light from ATP and luciferin. Luminescence was measured using a TD-20/20 luminometer. Chondrocytes were cultured at a density of 5 x 10^4 cells/well for 24 hours in 24-well plates and processed for ATP bioluminescence assays. Results were normalized to cellular protein concentration.

Treatment with ATP synthesis inhibitor - In vitro: 3-bromopyruvate (3-BrPA, Sigma), a strong alkylating agent that abolishes cell ATP production via the inhibition of both glycolysis and oxidative phosphorylation (25-27), was added at 10^{-6} M~10^{-5} M in the differentiation medium from day 1 to day 7. *In vivo*: 3-BrPA (20 μg/kg of body weight) was intraperitoneal injected daily for 10 days into C57BL/6J mice. Control mice received vehicle PBS.

Statistical Analysis - Data were presented as mean +/- SEM. Raw data were analyzed by Mann-Whitney's U test or one-way analysis of variance followed by a post hoc test (Fisher's projected least significant difference) (StatView, SAS Institute Inc., Cary, NC) with a significance level of $p < 0.05$.

RESULTS

Reduced apoptosis and mineralization in growth plate cartilage in Hyp mice - It has been reported that apoptosis is a prerequisite to mineralization of chondrocytes (28). Previous studies including ours have reported that the growth plate cartilage in *Hyp* mice is hypomineralized (5,6). We, therefore, examined apoptosis in the growth plate cartilage in *Hyp* mice compared to WT mice. Histological examination revealed that hypertrophic cartilage was elongated and disorganized in *Hyp* mice (Figure 1 A, left). In conjunction with this, TUNEL staining showed decreased apoptosis in hypertrophic cartilage in *Hyp* mice (Figure 1A, right and Figure 1B). Consistent with these *in vivo* results, chondrocytes isolated from *Hyp* mice (*Hyp* chondrocytes) in culture showed decreased apoptosis assessed by DNA fragmentation using a commercially-available ELISA kit (Figure 1C) and mineralization determined by alizarin red staining (Figure 1D, bottom). Quantification of alizarin red staining was shown in Figure 1F. However, GAG synthesis that takes place at an early stage of chondrogenesis was not altered in *Hyp* chondrocytes as determined by alcian blue staining (Figure 1D, top) Alcian blue staining was quantified in Figure 1E.

Cellular events involved in reduced apoptosis in Hyp chondrocytes - Since activation of caspase-9 and caspase-3 is an important step that leads to apoptosis, the activity of caspase-9 and caspase-3 was next determined in WT and *Hyp* chondrocytes in culture. The activity of caspase-9 (Figure 2A) and caspase-3 (Figure 2B) was significantly decreased in *Hyp* chondrocytes. Adenosine triphosphate (ATP) has been reported to be critical in the activation of caspase-9 and caspase-3 (29, 30). Accordingly, we determined intracellular ATP levels in WT and *Hyp* chondrocytes and found that intracellular ATP levels in *Hyp* chondrocytes were significantly reduced compared with WT chondrocytes (Figure 2C). Collectively, these results suggest that decreased ATP levels impaired caspase signals and following apoptosis in *Hyp* chondrocytes.

Disturbed Pi homeostasis in Hyp chondrocytes - It has been described that Pi (polyphosphate) is a source of ATP (31). Accordingly, we next examined whether Pi uptake was changed in *Hyp* chondrocytes. As expected, we found that Pi uptake was significantly less in *Hyp* chondrocytes than WT chondrocytes (Figure 3A). Since cellular Pi uptake is under the control of NPT (11), NPT expression in *Hyp* chondrocytes was subsequently determined. RT-PCR showed that the type III NPT *Pit-1* expression was decreased in *Hyp* chondrocytes (Figure 3B) and real-time PCR demonstrated *Pit-1* expression was reduced at early stages of chondrocyte culture (Figure 3C). Consistent with our results, previous studies also reported that an increase in *Pit-1* expression at early stage was associated with late chondrocyte differentiation (16, 18). On the other hand, there was no difference in the type II *Npt2a* expression between WT and *Hyp* chondrocyte (Figure 3B and Figure 3D). The type I *Npt1* expression was not

detected in WT and *Hyp* chondrocytes (Figure 3B). These results suggest that Pi uptake via *Pit-1* is specifically involved in the regulation of chondrogenesis including apoptosis and mineralization.

Suppression of chondrocyte differentiation by NPT inhibitor - To verify whether a decrease in Pi uptake due to reduced *Pit-1* expression is responsible for a reduction in ATP levels in *Hyp* chondrocytes, we determined the effects of phosphonoformic acid (PFA or foscarnet), which is a competitive inhibitor of Pi uptake via NPT (23), on intracellular ATP levels. PFA (10^{-5}-10^{-3} M) reduced Pi-uptake in chondrocytes in a dose-dependent manner (data not shown). PFA (10^{-5} M) profoundly reduced intracellular ATP levels (Figure 4A). Of note, PFA treatment caused disorganization of growth plate cartilage (Figure 4B, left) and significantly decreased the number of TUNEL-positive chondrocytes in the hypertrophic cartilage (Figure 4B, right and Figure 4C) in a similar manner to those seen in *Hyp* mice. Consistent with these *in vivo* results, PFA markedly inhibited mineralization of chondrocytes in a dose-dependent manner (Figure 4D, bottom and 4E), while GAG synthesis was not affected by PFA treatment (Figure 4D, top). Furthermore, PFA also inhibited caspase-9 (Figure 4F) and caspase-3 activity (Figure 4G). We determined serum Pi levels in PFA-treated mice. There was a trend of decreased serum Pi levels in PFA-treated mice but it was not significantly different (Figure 4H). The results are consistent with the notion that Pi uptake via *Pit-1* is closely associated with late chondrogenesis including apoptosis and mineralization through reducing ATP synthesis. These results also suggest an important role for intracellular Pi over extracellular Pi in the regulation of apoptosis and ATP synthesis in chondrocytes.

Suppression of chondrocyte differentiation by NPT siRNA - To further and more specifically verify the role of *Pit-1* on chondrocyte differentiation, we performed knock-down experiments using small interfering RNA (siRNA) for *Pit-1*. As control, *Npt2a* was also knocked-down. siPit-1 and siNpt2a profoundly reduced *Pit-1* and *Npt2a* mRNA levels in WT chondrocytes, respectively (Figure 5A). *Pit-1* knock-down by siPit-1 significantly decreased Pi-uptake (Figure 5B), intracellular ATP levels (Figure 5C), caspase-9 (Figure 5D) and caspase-3 activity (Figure 5E). In parallel with these, apoptosis (Figure 5F) and mineralization (Figure 5G and 5H) were also suppressed. In contrast, knock-down of *Npt2a* by siNpt2a had no effects on apoptosis and mineralization and other determinations (Figure 5B, 5C, 5D, 5E, 5F, 5G, and 5H). These data suggest that *Pit-1* specifically controls Pi uptake and following cascades of ATP-dependent caspase signaling, apoptosis and mineralization in chondrocytes.

Recovery of differentiation in Hyp chondrocytes by Pit-1 overexpression - As an alternative approach to confirm a critical role of *Pit-1* in apoptosis and mineralization in chondrocytes, we next examined the effects of *Pit-1* overexpression on *Hyp* chondrocytes. *Pit-1* overexpression significantly increased Pi uptake (Figure 6A) and intracellular ATP levels (Figure 6B) in *Hyp* chondrocytes. Furthermore, *Pit-1* overexpression also stimulated caspase-9 (Figure 6C) and caspase-3 activity (Figure 6D), apoptosis (Figure 6E) and mineralization (Figure 6F and 6G). WT chondrocytes also showed significantly increased Pi uptake (Figure 6A), intracellular ATP levels (Figure 6B), caspase-9 (Figure 6C) and caspase-3 activity (Figure 6D), apoptosis (Figure 6E) and mineralization (Figure 6F and 6G) by *Pit-1* overexpression. These results further suggest that *Pit-1* is critical in the regulation of Pi uptake and following cascades of ATP-dependent caspase signaling, apoptosis and mineralization in chondrocytes.

Suppression of chondrocyte differentiation by ATP synthesis inhibitor - To further examine the role of intracellular ATP in chondrocyte differentiation, we studied the effects of the ATP synthesis inhibitor 3-bromopyruvate (3-BrPA). 3-BrPA (10^{-6}M) significantly reduced intracellular ATP levels in WT chondrocytes in culture (data not shown). Caspase-9 (Figure 7A) and caspase-3 activity (Figure 7B) were also significantly decreased in 3-BrPA-treated chondrocytes. More importantly, 3-BrPA treatment significantly decreased the number of TUNEL-positive chondrocytes in the hypertrophic zone in mice (Figure 7C and Figure 7D). 3-BrPA inhibited chondrocyte mineralization in a dose-dependent manner (Figure 7E and 7F). However, GAG synthesis was not affected by 3-BrPA (Figure 7E). The serum Pi levels in 3-BrPA-treated mice were not significantly different from control mice (Figure 7G), suggesting an important role for intracellular Pi over extracellular Pi. These results suggest that ATP synthesis is important for chondrocytes to undergo apoptosis via caspase signaling and advance to mineralization.

DISCUSSION

In the present study, we explored the role of Pi/NPT system in chondrogenesis using *Hyp* mice compared with WT mice. We found that *Hyp* mice exhibited a widened and disorganized hypertrophic zone with reduced chondrocyte apoptosis compared with WT mice. In addition, PFA (a competitive inhibitor of *Pit-1*) or 3-BrPA (an ATP synthesis inhibitor) markedly caused elongation and disorganization of hypertrophic cartilage with reduced apoptosis in WT mice in a similar manner to *Hyp* mice. It is noted that the disorders in the hypertrophic zone were most severe in *Hyp* mice compared with PFA- or 3-BrPA-treated mice, despite that the number of TUNEL-positive cells are comparable in these mice. We postulate that the disorders in *Hyp* mice are congenital and irreversible and thus most severe, whereas the disorders seen in PFA- and 3-BrPA-treated mice are due to transient exposure of these agents and reversible and thus less severe.

Consistent with these *in vivo* results, *Hyp* chondrocytes in culture exhibited decreased activity of the apoptotic signaling including caspase-9 and caspase-3 and apoptosis and mineralization following to reduced Pi uptake and cellular ATP synthesis. Furthermore, PFA or 3-BrPA diminished caspase-9 and caspase-3 activity, apoptosis and mineralization in conjunction with a reduction in Pi uptake and ATP synthesis in WT chondrocytes. *Hyp* primary chondrocytes displayed a decrease in *Pit-1* (type III NPT) mRNA expression compared with WT chondrocytes, while there was no difference in type IIa NPT mRNA expression between WT and *Hyp* chondrocytes. WT and *Hyp* chondrocytes expressed no type I NPT mRNA. Meanwhile, GAG synthesis, which is an early event in chondrogenesis, was not reduced in *Hyp* chondrocytes and PFA and 3-BrPA or knockdown of *Pit-1* failed to decrease GAG synthesis in WT chondrocytes. *Pit-1* overexpression restored apoptosis and mineralization in *Hyp* chondrocytes. Taken together, these results suggest that Pi uptake via *Pit-1* and consequent ATP synthesis are critical in the regulation of late chondrogenesis including apoptosis and mineralization. These results also suggest that the disruption of cellular Pi homeostasis causes abnormal endochondral ossification due to a reduction of ATP synthesis in Hyp mice. In support of our study, Zalutskaya et al (32) have recently described that Pi activates mitochondrial apoptotic pathways and promotes endochondral ossification.

ATP synthesis and chondrogenesis - A notable and novel finding obtained in this study is that 3-BrPA inhibits apoptosis and mineralization in growth plate hypertrophic cartilage *in vivo* and primary chondrocytes *in vitro*. 3-BrPA is an alkylating agent that decreases cellular ATP via inhibition of hexokinase in glycolysis and is shown to promote cancer cell death through activation of mitochondrial pathway of apoptosis or necrosis (33). Of note, ATP-depleting effect of 3-BrPA is prominent only in tumor cells but not apparent in non-transformed cells (34). Hence, it has been proposed that 3-BrPA could be an anti-cancer agent for varieties of cancers. In addition to these effects on cancers, our results show that 3-BrPA inhibits the differentiation of cartilage, suggesting that ATP generation is also necessary for non-transformed chondrocytes to differentiate and that chondrogenesis is thus an energy-dependent biological event.

Decreased Pit-1 expression and Hyp skeletal phenotype - Decreased Pi-uptake in *Hyp* chondrocytes is likely primarily due to reduced *Pit-1* mRNA expression. Type IIa NPT expression was not diminished in *Hyp* chondrocytes and type I NPT was not expressed in chondrocytes. Earlier reports described that disturbed endochondral ossification was not rescued by Pi supplementation in *Hyp* mice (35-37), suggesting that intrinsic factors are involved. Miao et al (5) showed that reduced expression of PHEX and MMP-9 was associated with cartilage abnormalities in *Hyp* mice. Our results suggest that *Pit-1* is one of these intrinsic factors responsible for the abnormal chondrogenesis seen in *Hyp* mice as well.

Regulation of Pit-1 expression - The mechanism underlying down-regulation of *Pit-1* expression in *Hyp* chondrocytes is unknown. Recent studies have reported that stanniocalcin 1 (STC1) increases *Pit-1* mRNA expression in osteoblasts (38) and STC1 and STC2 have been shown to regulate Pi-uptake in chicken chondrocytes (39). STC1 stimulates renal Pi uptake and increases *Pit1* expression in osteoblasts (40), whereas STC2 inhibits the *Pit1* expression and renal Pi uptake (38). Thus, STC1 and STC2 have an opposite action in the regulation of *Pit-1* expression. Therefore, it is intriguing to examine whether STC1 or STC2 is involved in the *Pit-1* expression in chondrocytes. In preliminary experiments, we determined the expression of *Stc1* and *Stc2* mRNA in WT and *Hyp* chondrocytes using RT-PCR and real-time PCR. The *Stc2 mRNA* was expressed in both WT and *Hyp* chondrocytes at the same level (data not shown). However, the expression of *Stc1 mRNA* was decreased in *Hyp*

chondrocytes compared with WT chondrocytes (data not shown). These results suggest that STC1 but not STC2 regulates *Pit-1* expression in chondrocytes.

Involvement of fibroblast growth factor23 - Fibroblast growth factor 23 (FGF23) is a hormone that regulates serum Pi levels (41). FGF23 requires Klotho for its signaling as the co-receptors in addition to the canonical FGFR1(IIIc) (42, 43). Mice transgenic for FGF23 displayed a reduction in *Npt2a* expression in the renal proximal tubules (44), indicating that FGF23 is a negative regulator of *Npt2a* expression, raising the possibility that Klotho-dependent FGF23 signaling regulates *Pit-1* expression in chondrocytes as well. FGF23 expression was predominantly localized in osteoblasts, cementoblasts, and odontoblasts, with a sporadic expression in some chondrocytes, osteocytes and cementocytes (45). However, we were not able to demonstrate FGF23 expression in primary mouse chondrocytes by RT-PCR. Further studies are needed to elucidate the relationship between FGF23 signaling and *Pit-1* expression in cartilage.

In conclusion, we have found in the present study that chondrogenesis is modulated by cellular Pi uptake via Pit-1 and cellular ATP synthesis and thus is a biological event that depends on mitochondrial energy generation. We believe that these findings should provide us with a novel concept and alternative approaches to study the cellular differentiation that occurs in physiological conditions and also to analyze the skeletal abnormalities seen in congenital hypophosphatemic disorders such as XLH.

FOOTNOTES

We thank Dr. Kenichi Miyamoto and Dr. Hiroko Segawa (University of Tokushima Graduate School, Tokushima, Japan) for the kind gift of mouse *Pit-1* cDNA. This work was partly supported by the 21st Century COE program entitled "Origination of Frontier BioDentistry" at Osaka University Graduate School of Dentistry, supported by the Ministry of Education, Culture, Sports, Science and Technology and by Grants-in-Aid for Scientific Research from the Japanese Society for the Promotion of Science (T.Y. #A202290100).

The abbreviations used are: XLH, X-linked hypophosphatemia; Pi, phosphate; GAG, glycosaminoglycans; *Npt2a*, type IIa sodium-dependent Pi transporter; RT-PCR, Reverse transcription-polymerase chain reaction; PFA, phosphonoformic acid; ip, intraperitoneal injection; DAPI, 4',6-Diamidino-2-phenylindole; 3-BrPA, 3-Bromopyruvate; WT, wild-type; STC, Stanniocalcin; FGF23, fibroblast growth factor 23; ATPase, adenosine triphosphatase.

REFERENCES

1. Zuscik, M. J., Hilton, M. J., Zhang, X., Chen, D., and O'Keefe, R. J. (2008) *J Clin Invest* **118**(2), 429-438
2. Winters, R. W., Graham, J. B., Williams, T. F., Mc, F. V., and Burnett, C. H. (1958) *Medicine (Baltimore)* **37**(2), 97-142
3. Holm, I. A., Huang, X., and Kunkel, L. M. (1997) *Am J Hum Genet* **60**(4), 790-797
4. Eicher, E. M., Southard, J. L., Scriver, C. R., and Glorieux, F. H. (1976) *Proc Natl Acad Sci U S A* **73**(12), 4667-4671
5. Miao, D., Bai, X., Panda, D. K., Karaplis, A. C., Goltzman, D., and McKee, M. D. (2004) *Bone* **34**(4), 638-647.
6. Hayashibara, T., Hiraga, T., Sugita, A., Wang, L., Hata, K., Ooshima, T., and Yoneda, T. (2007) *J Bone Miner Res* **22**(11), 1743-1751
7. Boyde, A., and Shapiro, I. M. (1980) *Histochemistry* **69**(1), 85-94.
8. Kakuta, S., Golub, E. E., and Shapiro, I. M. (1985) *Calcif Tissue Int* **37**(3), 293-299.
9. Mwale, F., Tchetina, E., Wu, C. W., and Poole, A. R. (2002) *J Bone Miner Res* **17**(2), 275-283.
10. Shapiro, I. M., and Boyde, A. (1984) *Metab Bone Dis Relat Res* **5**(6), 317-326.
11. Virkki, L. V., Biber, J., Murer, H., and Forster, I. C. (2007) *Am J Physiol Renal Physiol* **293**(3), F643-654
12. Palmer, G., Zhao, J., Bonjour, J., Hofstetter, W., and Caverzasio, J. (1999) *Bone* **24**(1), 1-7.
13. Mansfield, K., Teixeira, C. C., Adams, C. S., and Shapiro, I. M. (2001) *Bone* **28**(1), 1-8.
14. Cecil, D. L., Rose, D. M., Terkeltaub, R., and Liu-Bryan, R. (2005) *Arthritis Rheum* **52**(1), 144-154.

15. Fujita, T., Meguro, T., Izumo, N., Yasutomi, C., Fukuyama, R., Nakamuta, H., and Koida, M. (2001) *Jpn J Pharmacol* **85**(3), 278-281.
16. Guicheux, J., Palmer, G., Shukunami, C., Hiraki, Y., Bonjour, J. P., and Caverzasio, J. (2000) *Bone* **27**(1), 69-74.
17. Montessuit, C., Caverzasio, J., and Bonjour, J. P. (1991) *J Biol Chem* **266**(27), 17791-17797.
18. Wang, D., Canaff, L., Davidson, D., Corluka, A., Liu, H., Hendy, G. N., and Henderson, J. E. (2001) *J Biol Chem* **276**(36), 33995-34005
19. Wu, L. N., Guo, Y., Genge, B. R., Ishikawa, Y., and Wuthier, R. E. (2002) *J Cell Biochem* **86**(3), 475-489
20. Magne, D., Bluteau, G., Faucheux, C., Palmer, G., Vignes-Colombeix, C., Pilet, P., Rouillon, T., Caverzasio, J., Weiss, P., Daculsi, G., and Guicheux, J. (2003) *J Bone Miner Res* **18**(8), 1430-1442.
21. Shimomura, Y., Yoneda, T., and Suzuki, F. (1975) *Calcif Tissue Res* **19**(3), 179-187
22. Rowe, P. S., Ong, A. C., Cockerill, F. J., Goulding, J. N., and Hewison, M. (1996) *Bone* **18**(2), 159-169.
23. Loghman-Adham, M. (1996) *Gen Pharmacol* **27**(2), 305-312
24. Swenson. C.L., Weisbrode, S.E., Nagode, L.A., Hayes, K.A., Steinmeyer, C.L., Mathes, L.E. (1991) *Calcif Tissue Int* **48**(5), 353-361.
25. Geschwind, J. F., Ko, Y. H., Torbenson, M. S., Magee, C., and Pedersen, P. L. (2002) *Cancer Res* **62**(14), 3909-3913.
26. Jones, A. R., Gillan, L., and Milmlow, D. (1995) *Contraception* **52**(5), 317-320.
27. Ko, Y. H., Smith, B. L., Wang, Y., Pomper, M. G., Rini, D. A., Torbenson, M. S., Hullihen, J., and Pedersen, P. L. (2004) *Biochem Biophys Res Commun* **324**(1), 269-275.
28. Gibson, G. (1998) *Microsc Res Tech* **43**(2), 191-204
29. Eguchi, Y., Srinivasan, A., Tomaselli, K. J., Shimizu, S., and Tsujimoto, Y. (1999) *Cancer Res* **59**(9), 2174-2181.
30. Li, P., Nijhawan, D., Budihardjo, I., Srinivasula, S. M., Ahmad, M., Alnemri, E. S., and Wang, X. (1997) *Cell* **91**(4), 479-489.
31. Rao, N. N., Gomez-Garcia, M. R., and Kornberg, A. (2009) *Annu Rev Biochem* **78**, 605-647
32. Zalutskaya, A. A., Cox, M. K., and Demay, M. B. (2009) *J Cell Biochem* **108**(3), 668-674
33. Pelicano, H., Martin, D. S., Xu, R. H., and Huang, P. (2006) *Oncogene* **25**(34), 4633-4646
34. Xu, R. H., Pelicano, H., Zhou, Y., Carew, J. S., Feng, L., Bhalla, K. N., Keating, M. J., and Huang, P. (2005) *Cancer Res* **65**(2), 613-621
35. Ecarot, B., Glorieux, F. H., Desbarats, M., Travers, R., and Labelle, L. (1992) *J Bone Miner Res* **7**(5), 523-530.
36. Tanaka, H., Seino, Y., Shima, M., Yamaoka, K., Yabuuchi, H., Yoshikawa, H., Masuhara, K., Takaoka, K., and Ono, K. (1988) *Bone Miner* **4**(3), 237-246
37. Yoshikawa, H., Masuhara, K., Takaoka, K., Ono, K., Tanaka, H., and Seino, Y. (1985) *Bone* **6**(4), 235-239
38. Yoshiko, Y., Candeliere, G. A., Maeda, N., and Aubin, J. E. (2007) *Mol Cell Biol* **27**(12), 4465-4474. Epub 2007 Apr 4416.
39. Wu, S., Yoshiko, Y., and De Luca, F. (2006) *J Biol Chem* **281**(8), 5120-5127. Epub 2005 Dec 5123.
40. Ishibashi, K., and Imai, M. (2002) *Am J Physiol Renal Physiol* **282**(3), F367-375
41. Fukumoto, S., and Yamashita, T. (2007) *Bone* **40**(5), 1190-1195
42. Kurosu, H., Ogawa, Y., Miyoshi, M., Yamamoto, M., Nandi, A., Rosenblatt, K. P., Baum, M. G., Schiavi, S., Hu, M. C., Moe, O. W., and Kuro-o, M. (2006) *J Biol Chem* **281**(10), 6120-6123. Epub 2006 Jan 6125.
43. Urakawa, I., Yamazaki, Y., Shimada, T., Iijima, K., Hasegawa, H., Okawa, K., Fujita, T., Fukumoto, S., and Yamashita, T. (2006) *Nature* **444**(7120), 770-774
44. Shimada, T., Urakawa, I., Yamazaki, Y., Hasegawa, H., Hino, R., Yoneya, T., Takeuchi, Y., Fujita, T., Fukumoto, S., and Yamashita, T. (2004) *Biochem Biophys Res Commun* **314**(2), 409-414.
45. Yoshiko, Y., Wang, H., Minamizaki, T., Ijuin, C., Yamamoto, R., Suemune, S., Kozai, K., Tanne, K., Aubin, J. E., and Maeda, N. (2007) *Bone* **40**(6), 1565-1573

FIGURE LEGENDS

FIGURE 1. Apoptosis and related events in *Hyp* chondrocytes. *A*, Histological examination of chondrocyte apoptosis. Hematoxylin/eosin staining (left) and TUNEL staining (right) were performed using tibiae of 4-week-old WT and *Hyp* mice. Hypertrophic zone is marked with dotted line and scale bar indicates 200 μm. Representative pictures obtained out of numerous sections of four mice from each group are shown. *B*, Number of TUNEL-positive cells in tibial growth plate of WT and *Hyp* mice. *C*, Quantitative determination of chondrocyte apoptosis. Cells were cultured in the differentiation medium in 96-well plates for 7days. The determination was conducted using the Cell Death Detection ELISA PLUS after differentiation. Data are shown as apoptotic activity. *D*, Histochemical staining of WT and *Hyp* chondrocytes. Cells were cultured for 7days in the differentiation medium and stained with alcian blue for GAG synthesis (top) and with alizarin red-S for mineralization (bottom). *E*, Quantification of alcian blue staining. *F*, Quantification of alizarin red staining. Results are expressed as mean +/- SEM of four separate experiments. *Significantly different from WT chondrocytes ($p<0.05$).

FIGURE 2. Activity of apoptotic signaling pathways. *A*, Caspase-9 activity in WT and *Hyp* chondrocytes. *B*, Caspase-3 activity in WT and *Hyp* chondrocytes. Activity was measured using the Caspase-Glo 9 and Caspase-Glo 3/7 assay kit after differentiation. *C*, Intracellular ATP levels in WT and *Hyp* chondrocytes. Cells were cultured at a density of 1 x 10^4 cells/well in 96-well plates for 24 hours. ATP levels were measured using the ATP assay kit.

FIGURE 3. Characterization of *Hyp* chondrocytes. *A*, Time-course of Pi uptake in WT (open circle) and *Hyp* (solid circle) chondrocytes. Cells were cultured for 7days in the differentiation medium and Pi uptake was determined as described in Experimental Procedures. *B*, Expressions of *Npt*1, *Npt2a* and *Pit-1* mRNA in WT and *Hyp* chondrocytes. Total RNA isolated from chondrocytes cultured for 24 hours was used for RT-PCR analysis using the primer pairs. β-actin was amplified as control. *C*, Time-dependent expression of *Pit-1* mRNA by real-time PCR. *D*, Time-dependent expression of *Npt2a* mRNA by real-time PCR. The amount of *Npt2a* and *Pit-1* of WT chondrocytes at day 0 was designated as 1.0 and normalized to GAPDH. Results are expressed as mean +/- SEM of four separate experiments. *Significantly different from WT chondrocytes ($p<0.05$).

FIGURE 4. Effects of PFA on chondrocyte differentiation. *A*, Intracellular ATP levels. Cells were cultured in the presence of 10^{-5}M PFA. ATP levels were measured using the ATP assay kit. *B*, Histological examination of chondrocyte apoptosis. Hematoxylin/eosin staining (left) and TUNEL staining (right) were performed on tibial sections from 31-day-old control and PFA-treated mice. Hypertrophic zone is marked with dotted line and scale bar indicates 200 μm. Representative pictures obtained out of numerous sections of four mice from each group are shown. *C*, Number of TUNEL positive cells in tibial growth plate of control and PFA-treated mice. *D*, Histochemical staining of chondrocytes. Cells were cultured in the presence of 10^{-5} M PFA and stained with alcian blue for GAG synthesis (top) and alizarin red-S for mineralization (bottom). *E*, Quantification of alizarin red staining. *F*, Caspase-9 activity. *G*, Caspase-3 activity. Cells were cultured in the presence of 10^{-5}M PFA. Activity was measured using the Caspase-Glo 9 and Caspase-Glo 3/7 assay. *H*, Serum Pi levels. Results are expressed as mean +/- SEM of four separate determinations. *Significantly different from control ($p<0.05$).

FIGURE 5. *Npt2a* and *Pit-1* knockdown by siRNA in chondrocytes. *A*, siRNA for siNEGATIVE (Control), siNPT2a or siPIT-1 was transfected in chondrocytes and the expression of *NPT2a*, *Pit-1* or GAPDH was analyzed by RT-PCR. *B*, Pi-uptake in siNEGATIVE- (Control), siNPT2a- and siPIT-1-transfected chondrocytes was determined in the presence of 3 μCi/mL of $KH_2{}^{32}PO_4$. *C*, Intracellular ATP levels in siNEGATIVE- (Control), siNPT2a- and siPIT-1-transfected chondrocytes. *D*, Caspase-9 activity in siNEGATIVE- (Control), siNPT2a- and siPIT-1-transfected chondrocytes. *E*, Caspase-3 activity in siNEGATIVE- (Control), siNPT2a- and siPIT-1-transfected chondrocytes. *F*, Quantitative determination of chondrocyte apoptosis in siNEGATIVE- (Control), siNPT2a- and siPIT-1-transfected chondrocytes. *G*, Histochemical staining of siNEGATIVE- (Control), siNPT2a- and siPIT-1-transfected chondrocytes. Cells were cultured and stained with alcian blue for GAG synthesis (top) and alizarin red-S for mineralization (bottom). *H*, Quantification of alizarin red staining. We repeated the experiments twice using different preparation of primary chondrocytes and obtained the identical results. Results are expressed as mean +/- SEM of two separate determinations.*Significantly different from control ($p<0.05$).

FIGURE 6. Effects of *Pit-1* overexpression in chondrocytes. *A*, Empty vector (Control) or *Pit-1* was transfected in WT and *Hyp* chondrocytes. Pi-uptake was determined in the presence of 3 μCi/mL of $KH_2{}^{32}PO_4$. *B*, Intracellular ATP levels in Control or *Pit-1*-transfected WT and *Hyp* chondrocytes. *C*, Caspase-9 activity in control and *Pit-1*-transfected WT and *Hyp* chondrocytes. *D*, Caspase-3 activity in control and *Pit-1*-transfected WT and *Hyp* chondrocytes. *E*, Quantitative determination of apoptosis in control and *Pit-1*-transfected WT and *Hyp* chondrocytes. *F*, Histochemical staining of control and *Pit-1*-transfected WT and *Hyp* chondrocytes. Cells were cultured and stained with alizarin red-S for mineralization. *Pit-1* expression was confirmed by RT-PCR. *G*, Quantification of alizarin red staining. We repeated the experiments twice using different preparation of primary chondrocytes and obtained the identical results. Results are expressed as mean +/- SEM of two separate determinations. *Significantly different from WT control ($p<0.05$). $^{+}$Significantly different from *Hyp* control ($p<0.05$).

FIGURE 7. Effects of 3-BrPA on chondrocyte apoptosis and calcification. *A*, Effects of 3-BrPA on caspase-9 activity. *B*, Effects of 3-BrPA on caspase-3 activity. Cells were treated with 10^{-6} M 3-BrPA for 7 days and measured for caspase activity. *C*, Histological examination of chondrocyte apoptosis. Hematoxylin/eosin staining (left) and TUNEL staining (right) were performed on tibial sections from 31-day-old control and 3-BrPA-treated mice. Hypertrophic zone is marked with dotted line and scale bar indicates 200 μm. *D*, Number of TUNEL-positive cells in tibial growth plate of control and 3-BrPA-treated mice. *E*, Histochemical staining of chondrocytes. Cells were cultured for 7days in the presence of 10^{-6} and 10^{-5} M 3-BrPA and stained with alcian blue for GAG synthesis (top) and alizarin red-S for mineralization (bottom). *G*, Quantification of alizarin red staining. *H*, Serum Pi levels. Results are expressed as mean +/- SEM of four separate experiments. *Significantly different from control ($p<0.05$).

Figure 1

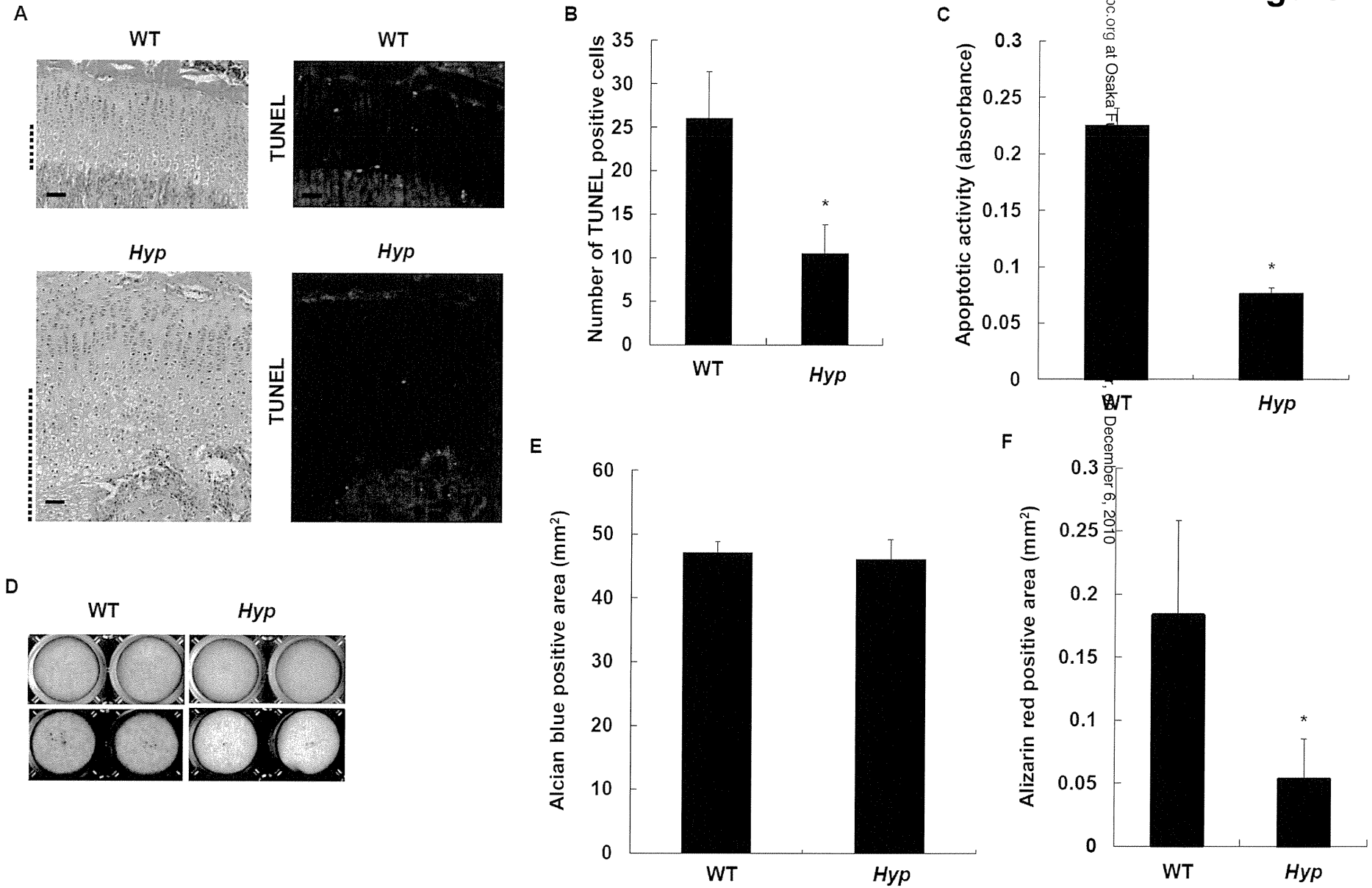

Figure 2

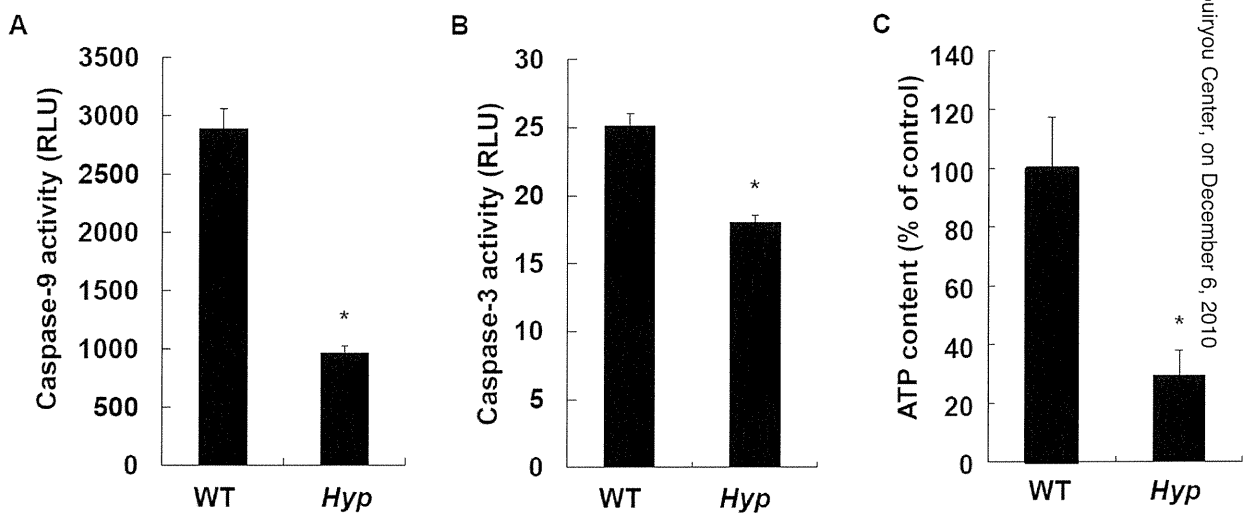

Figure 3

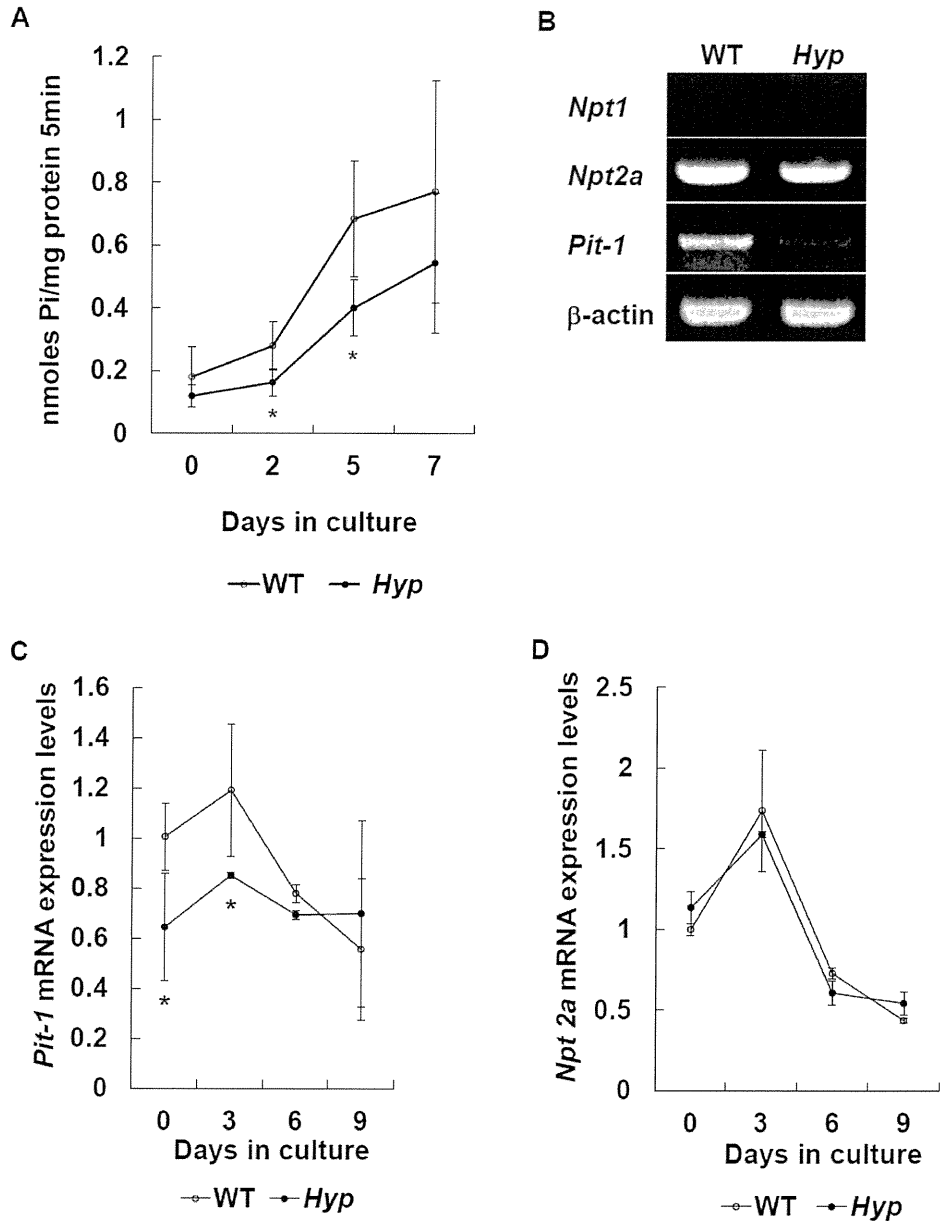

Figure 4